

# Analysis of Deformation Characteristics of Magnesium AZ80 Wrought Alloy under Hot Conditions

Dominik Kobold<sup>1,\*</sup> - Tomaž Pepelnjak<sup>2</sup> - Gašper Gantar<sup>1</sup> - Karl Kuzman<sup>2</sup>

<sup>1</sup>TECOS Slovenian Tool and Die Development Centre, Slovenia

<sup>2</sup>University of Ljubljana, Faculty of Mechanical Engineering, Slovenia

*Light-weight and environmentally friendly materials with good mechanical properties are much appreciated in various modern applications. Weight reduction can improve the performance of many components while reducing the fuel consumption of vehicles.*

*Magnesium is one of the most popular weight-reducing materials because of its low density, good mechanical properties, large natural reserves and good machining properties. The strength, stiffness and favourable metallographic structure of products can be improved by a forging process in which components are shaped from feedstock slugs by applying compressive force through various forging dies. However, widespread usage of forging technology in industrial practice is very rare in comparison to casting, due to the specific deformation characteristics of magnesium having a hexagonal close packed basal crystal structure.*

*This paper deals with the determination of the influence of the most important process parameters on the deformation process of magnesium alloys. On the basis of extensive experimental study, anisotropic flow and the impact of the most important input process factors on the plastic deformation of AZ80 wrought alloy are considered. The results presented in this paper are directly related to industrial practice and have significant potential as a case study for the further development of FEM models capable of predicting anisotropic material flow during applied plastic deformation. The studies presented in the paper also make possible defining recommended technological parameters of the forging process.*

©2010 Journal of Mechanical Engineering. All rights reserved.

**Keywords:** magnesium forging, anisotropy, plastic deformation, flow curves, AZ80, wrought magnesium alloys

## 0 INTRODUCTION

In recent years, light-weight design has become even more important due to several benefits relating to improvements of the performances of many applications. Low density, good mechanical properties, recycling possibilities and (not the least) competitive price play important roles in the selection of the product's material.

Since magnesium alloys are the lightest engineering metallic materials having good mechanical properties comparable to aluminium alloys [1], vast potential for use has been found in many different engineering applications in which weight is extremely important. However, in order to meet commitments to reduce the fuel consumption of vehicles, widespread usage of magnesium components in automotive industry is expected in the short-term future [1] and [2].

Nowadays, high-pressure die casting of magnesium alloys is mostly in use due to its high

productivity and the possibility of producing complex net-shape products. However, due to the high cost of casting machines and dies, only the production of large series is reasonable. Due to low mechanical properties and material porosity of casted products, (hot) forging can be a more appropriate technique for producing of structural magnesium components. Specifically, hot forging has been regarded as one of the main processing techniques enabling net-shape production and the possibility of obtaining high deformation combined with very good mechanical properties of products [3].

Despite the benefits, the forging of magnesium alloys is rarely in use in industrial practice due to specific deformation characteristics as well as a lack of know-how and practical experience related to deformation behaviour in applied plastic deformation.

However, proper design of the robust forming process needs consideration of many initial process parameters (material, machines

\*Corr. Author's Address: TECOS Slovenian Tool and Die Development Centre, Kidričeva 25, 3000 Celje, Slovenia, dominik.kobold@tecos.si

types and settings, CAD models, tools, initial temperatures, ram speeds etc.) to provide tailored and cost-efficient technologies for the production of components.

This paper deals with a study for the determination of the influence of various process parameters on the deformation process and anisotropic flow during compression loading conditions. The studies presented in the paper also make possible defining recommended process parameters of the forging process and also have significant potential for industrial use.

## 1 BACKGROUND

It is generally known that magnesium has a hexagonal close packed (h. c. p.) basal crystal lattice with a significant effect on plastic deformation. For h. c. p., it is typical that plastic deformation applied in a conventional way at room temperature is not possible, because only slips of basal crystal planes (0001) are available [4]. At temperatures above 230 °C [5], formations of additional prismatic and pyramidal gliding planes as well as a twinning mechanism enable sufficient plastic deformation [4] to [6]. Moreover, the formation of gliding mechanisms depends on both on loading direction and on loading type (compression or tension, respectively), and causes anisotropic properties and asymmetry of yielding criterion as well [4].

Further, plastic deformation of magnesium as cast feedstock alloys is not possible due to too big crystal grains, with diameters from 200 to 400  $\mu\text{m}$ , usually formed during solidification and secondly, large material porosity [1]. Generally, during preparation of wrought feedstock alloys, a pre-deformation process (e.g. pre-extrusions) is essential for reducing grain sizes; however, it further affects anisotropic behaviour and material flow because texture with strong grain orientation is formed.

Metallographic analyses of AZ80 wrought alloy in T5 condition (artificial ageing at 170 to 180 °C, 12 to 24 hours) show large differences in microstructure regarding to the cross section of the extruded bar. In cross sections parallel to the extrusion axis (Fig. 1a), strong grain orientation with fibre segregation of the participation phase  $\text{Mg}_{17}\text{Al}_{12}$  between grain boundaries is observed. Energy-dispersive X-ray spectroscopy (EDX) was used for detection precipitation phase  $\text{Mg}_{17}\text{Al}_{12}$

[2] and [7]. The  $\text{Mg}_{17}\text{Al}_{12}$  phase strengthens the alloy and subsequently has significant influence on plastic deformation behaviour [2]. The metallographic structure in cross sections perpendicular to extrusion axis (Fig. 1b) is much more uniformly distributed across whole section without any fibre orientations as is observed in the longitudinal cross section [7]. It should be noted that the same alloy in the same state was used in further experimental investigations represented below in the paper.

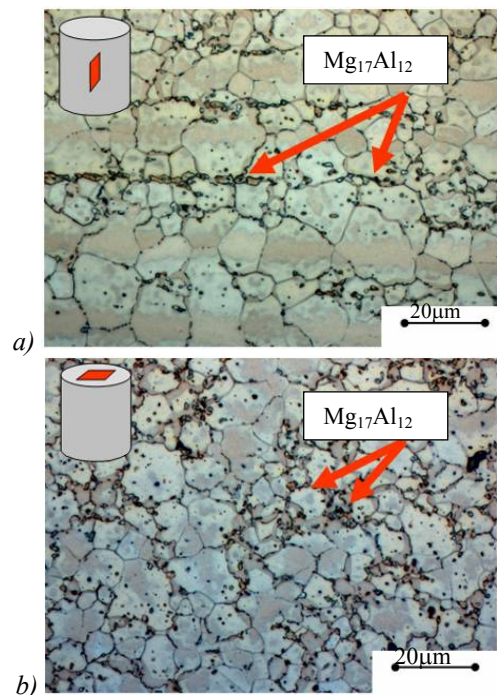


Fig. 1. AZ80 crystal metallographic structure a) longitudinal cross-section b) transverse cross-section [7]

Many authors deal with the problem of texture changes during the deformation process and determination of anisotropic characteristics of magnesium sheets or single crystals [4] to [6], but in fact, there is a major lack of studies dedicated to the consideration of the influence of process parameters on material flow in bulk forming of polycrystalline materials also having practical contributions that would make possible proper die cavities and slug design, as well as enabling the establishment of proper process parameters with the ultimate goal of ensuring the production of faultless parts with high repeatability.

2 EXPERIMENTAL PROCEDURES

As mentioned before, the AZ80 feedstock alloy in a T5 condition was investigated and studied for determination of anisotropic material flow and influence of process parameters on plastic deformation.

The basic characteristics of studied AZ80 feedstock alloy are represented in Table 1, where chemical composition is given, and in Table 2, where mechanical properties at room temperature are listed.

Table 1. Chemical composition of AZ80 commercial alloy [1]

Mark	Chemical composition [%]		
	Al	Zn	Mn
AZ80	7.8 – 9.2	0.2 – 0.8	0.12 – 0.5

Table 2: Mechanical properties of AZ80 commercial alloy in T5 condition [1]

Hardness [HB]	Strength [N/mm <sup>2</sup> ]		Elongation [%]
	R <sub>p0.2</sub>	R <sub>m</sub>	
69	180 – 215	290 – 315	5 – 8

2.1 Tests for Determination Anisotropic Material Flow

In order to make possible analyses of interactions between different process parameters, a statistical approach for the experiment design (DOE) has been used. A general full factorial DOE was chosen. It required minimally two replicates at unchanged process parameters, making possible analyses of standard errors due to deviations from average [8].

Process parameters were selected in accordance with the wide range of process parameters required in forging practice.

The AZ80 feedstock alloy used in this study was in the shape of a pre-extruded bar with 28 mm in diameter. An extruded bar is a good example of material having orthotropic mechanical characteristics which can be described by an assigned Cartesian orthogonal coordinate system. In our case, the x axis is designated along extrusion direction, while the other two axes perpendicular to the extrusion axis are denoted by y and z. These two axes denote directions with equal material properties and are therefore equivalent.

To consider different loading directions and eventual differences in material flow in each direction, cylindrical work-pieces (diameter of 16 mm and length of 20 mm) were machined from pre-extruded bar in longitudinal, transverse and in direction of 45° regarding the extrusion axis as shown in Fig. 2. The first process parameter (work-pieces orientation) has three levels in DOE. The choice of the simple shape of a cylindrical work-piece enables equivalent material flow in unrestricted directions during experiments and enables simple and effective comparison of the shapes after compression.

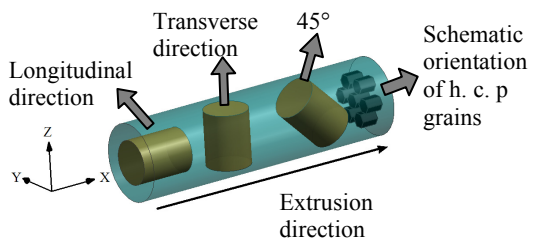


Fig. 2. Orientation of test work-pieces

The second process parameter was work-piece placement before compression. Two different placements were chosen: upright and radial as is shown in Fig. 3. Upright placement actually represents upsetting giving a simple deformation state while at radial compression or the so-called “cigar test”, a much more complex deformation state is achieved. At upsetting work-pieces were upset from height of 20 to 6.7 mm, while at radial compression work-pieces were compressed from the initial diameter of 16 mm to final thickness of 4 mm.

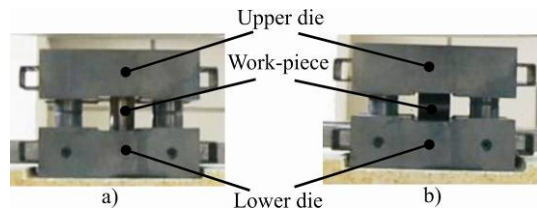


Fig. 3. Testing tool with inserted work-piece a) upright and b) radial placement

The third process parameter taken into account was initial work-piece temperature influencing deformability (forgeability) the most. It was selected and tested in three levels: 300 °C,

which is below the recommended temperature for plastic deformation of AZ80 alloy, 350 °C as the recommended temperature derived from literature [2] and 400 °C, which is above the recommended temperature.

The forth process parameter taken into account was ram speed ( $v_r$ ). To consider the influence of ram speed on deformation behaviour and material flow, two different velocities were chosen. The first at  $v_r = 5$  mm/s corresponded to slow and the second at  $v_r = 20$  mm/s to fast deformation.

Nevertheless, the ram speeds of forging hammers or screw presses are usually much faster, but due to characteristics of the hydraulic press used in experimental study, attaining faster ram speeds was limited.

Considering the interactions between work-pieces orientation on three levels, work-pieces placement on two levels, initial work-pieces temperature on three levels and ram speed on two levels according to the general factorial experiment design with three replicates at unchanged conditions required 108 experiments to be carried out. In Table 3, the main process parameters of the experimental process are listed, and the maximal logarithmic deformations and main strain rates are also calculated.

Table 3. Experimental process conditions

Material	AZ80 T5		
Work-piece dimension	diameter: $\phi 16_{-0}^{+0,02}$ mm height: $20_{-0}^{+0,02}$ mm		
Work-pieces orientation	longitudinal; transverse; 45°		
Work-piece placement	upright; radial		
Initial work-pieces temperatures	300 °C; 350 °C; 400 °C		
Ram speeds ( $v_r$ )	5 mm/s; 20mm/s		
Maximal log. deformation	upright: 1.09 radial: 1.37		
Mean strain rates ( $\dot{\phi}$ )		5 mm/s	20 mm/s
	upright	$0.4 \text{ s}^{-1}$	$1.6 \text{ s}^{-1}$
	radial	$0.57 \text{ s}^{-1}$	$2.3 \text{ s}^{-1}$
Replicates	3 at unchanged conditions		

The design of a special small testing tool consisting of upper and lower die each having

outer dimensions of  $95 \times 95 \times 27$  mm. The die's surfaces were also fine polished to  $R_{a(max)} = 0.05$   $\mu\text{m}$ . For each experiment testing tool with inserted work-piece (see Fig. 3) was put into the resistance-heated oven with an electro-controlled temperature field inside in order to enable isothermal testing. Typically, the testing tool together with the work-piece stayed inside the oven for 15 minutes. Before compression, the temperature of both dies and work-piece was checked using an electronic high-speed thermocouple to assure precise forging temperatures.

Constant temperature of testing tool during compression was also assured by using fireproof clay-block insulation between the lower die and press table, as shown in Fig. 4.

To reduce the friction between the die's and the work-piece's contact surfaces, an oil-based carbon lubricant emulsion (Thermex R7-271-03) was used.

Ram movement distance was measured with an inductive sensor mounted on the press while ram speed was controlled with an additional variable-flow restrictor valve. Data entry was automatic, carried out by a special-purpose computer program designed for real time measuring.

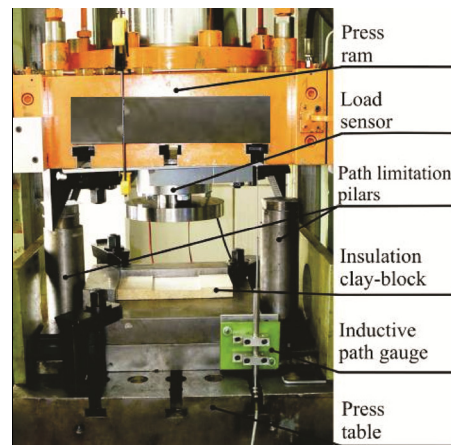


Fig. 4. Hydraulic press used for testing

The measured parameters on output were force-movement diagrams and shapes of compressed (forged) work-pieces. Force was measured continuously during the deformation by using a high precision 500 kN load sensor (type C450T) mounted between the hydraulic press ram

and testing tool. The shapes of the compressed work-pieces were measured with a 3D-optical digitalisation system (ATOS II). For measuring, two 35 mm camera lens and one 23 mm projector lens were used. Number of measuring points per individual scan was 1,300,000, achieved with camera resolution of  $1280 \times 1024$  pixels. The achieved measuring accuracy was within 0.015 mm [9].

### 3 ANALYSES OF RESULTS

#### 3.1 Mechanical Properties of Magnesium AZ80 Alloy

In order to better understand deformation behaviour, mechanical properties corresponding to various deformation conditions were also analysed with upsetting tests in previous experiments. Flow curves (true stress-strain curves) were obtained as functions of temperatures  $T$ , loading directions and strain rates  $\dot{\varphi}$  according to equivalent strains  $\varphi$  for exactly the same batch of feedstock material and in the same loading directions as is illustrated in Fig. 2 [10].

Cylindrical test specimens for determination flow curves had 10 mm in diameter and 15 mm in length. The temperature range taken into account was from 250 to 400 °C where the AZ80 alloy shows good formability with temperature increments of 50 °C and strain rates region  $\dot{\varphi}$  from 0.01 to 10 s<sup>-1</sup> with one decade increment, respectively [10].

Flow curves determined at various process parameters are presented in Fig. 5. From these charts, the vast dependencies of flow curves on process parameters and loading direction can be observed.

With the deformation of magnesium alloys, specifically AZ80, stress peak as a consequence of deformation hardening following by strong softening is apparent. At high strain rates above  $\dot{\varphi} = 1$  s<sup>-1</sup> stress peak is achieved at equivalent strain of  $\varphi \approx 0.2$ , while at lower strain rates, the stress peak is achieved at a strain range from  $\varphi \approx 0.05$  to 0.1 depending on temperature and loading direction. After deformation hardening, strong deformation softening follows to strain of  $\varphi \approx 0.6$  at high strain rates or to  $\varphi \approx 0.4$  at slow strain rates.

The reasons for such behaviour are probably in the formation of new gliding planes and twinning and, additionally, in dynamic recrystallisation, normally taking place at very slow strain rates [5].

Fig. 5a presents flow curves as a function of loading direction at constant temperature of 350 °C and strain rates of  $\dot{\varphi} = 10$  and 0.1 s<sup>-1</sup>. Particularly in the area where deformation hardening and softening occur (to equivalent strain of  $\varphi \approx 0.4$ ) especially at strain rate of  $\dot{\varphi} = 10$  s<sup>-1</sup>, major differences in flow curves regarding the loading direction are observed. The stress peaks are the highest in the longitudinal loading direction, followed by the transverse and direction of 45°. Such behaviour is a result of crystal grains orientation influencing the possibility of formation gliding planes and twinning mechanisms in h. c. p. polycrystalline materials.

Furthermore, differences between flow curves as a function of strain rates at a constant temperature are also large (Fig. 5b). With increasing of strain rates, the so-called deformation hardening/softening phenomena is significant since the higher the strain rate is, the bigger the yielding stress peak is observed.

In that point of view, the identified behaviour shows very unfavourable properties with significant risk for cracking at conditions in which very high strain rates are applied, which certainly happens at forming (forging) operations.

Furthermore, temperature play major role in the deformation process of magnesium alloys since sufficient plastic deformation is enabled only at elevated temperatures. Fig. 5c presents flow curves in the longitudinal loading direction as a function of temperature. With increased temperatures, yielding stresses are decreasing and (more importantly) stress peak is significant decreased as well. Nevertheless, plastic deformation at too high temperatures is not recommended due to the risk of hot cracking, as explained later.

Since mechanical properties have significant influence on plastic deformation, the represented flow curves show very clearly that the process window for forming of magnesium alloys is extremely narrow with only small allowed deviations from optimal process parameters.

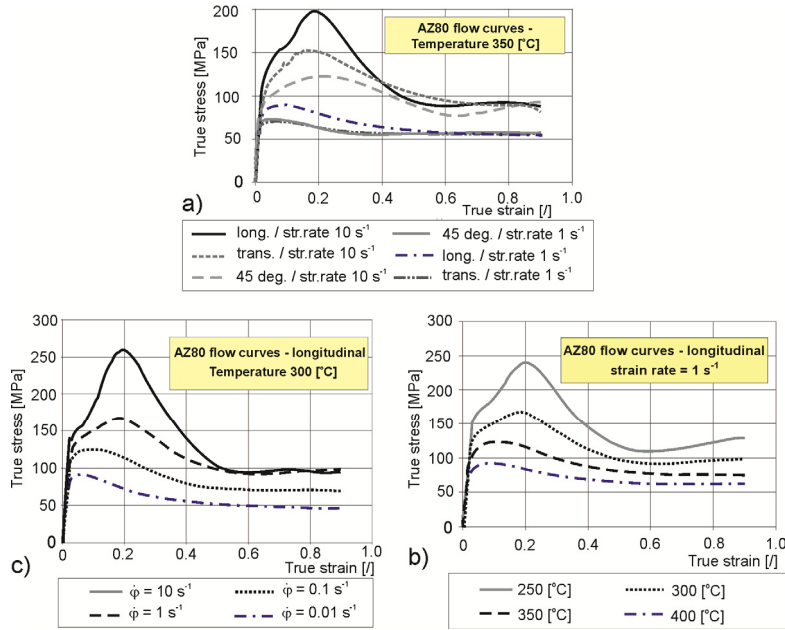


Fig. 5. Flow curves determined at various process parameters [10]

### 3.2 Upsetting Tests

Quite large differences between the shapes of the footprints have been observed at different process parameters (see Fig. 6). Cross-sections of work-pieces oriented in the 45° and transverse become elliptical as a consequence of anisotropic flow. Specifically, as is evident from flow curves, material flow is easier in the direction in which yielding stresses are lower rather than in the direction in which resistance against material flow is higher (greater yielding stresses).

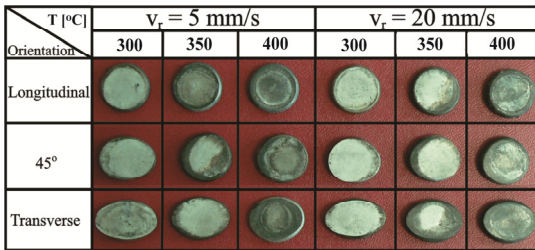


Fig. 6. Footprints of upset work-pieces

From analyses of the footprints' shapes, it can be assumed that formation of an elliptical shape is mainly affected by work-piece orientation, less so by initial work-piece

temperature, while ram speed has almost negligible influence.

There are well-established concepts for describing plastic anisotropy in sheet metals; however, in the field of bulk metal, there is a difference compared to sheet metal particular for materials having rotational symmetry (cylindrical orthotropy) as the extruded bars of AZ80 feedstock alloy studied in the present work have. The rotational symmetry is caused by crystallographic fibre texture along the extruded direction [11]. Below is a proposed mathematical evaluation of anisotropic flow at upsetting, based on the analogy of description anisotropy in sheet metals [12]. From the measurement of the principal axes of the ellipse, a mathematical function for evaluation of anisotropic material flow was proposed by introducing an axial anisotropy factor  $R_z$ . Factor  $R_z$  can be obtained by Eq. (1) [13]

$$R_z = \frac{\varphi_z}{\varphi_x}, \tag{1}$$

where  $\varphi_z$  and  $\varphi_x$  are the natural strains vertical and parallel to the extrusion axis and are obtained as following:

$$\varphi_z = \ln\left(\frac{D_2}{D_0}\right) \text{ and } \varphi_x = \ln\left(\frac{D_1}{D_0}\right), \tag{2}$$

where  $D_1$  and  $D_2$  are the axis of ellipse in two different directions (see Fig. 7) and  $D_0$  is an initial diameter of cylindrical work-piece [13].

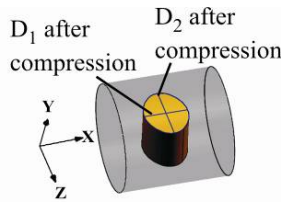


Fig. 7. Definition of  $D_1$  and  $D_2$  after upsetting

Unfortunately, as a consequence of friction between the work-piece and the die's contact surfaces, and especially due to inhomogeneous plastic deformation as a result of material anisotropic characteristics, the circumferential face of work-piece during upsetting is embossed, as shown on Fig. 8. To compensate for this, equivalent diameters  $D_1$  and  $D_2$  were calculated using Eq. (3). The equivalent diameter represents a measure between gravity centres of the cross section arcs of a work-piece (Fig. 8).

$$D_{1,2} = \frac{2D'' + D'}{3} \quad (3)$$

Fig. 8. Definition of  $D_1$  and  $D_2$  after upsetting

Statistical analysis of the impact of the studied process parameters on  $R_z$  is shown in Fig. 9 for a ram speed of 5 mm/s and in Fig. 10 for a ram speed of 20 mm/s. Box, triangle and deltoid on Figs. 9, 10, 14 and 15 represent arithmetic mean values of three measurements ( $R_z$  or  $L_1$  and  $L_2$ ) at a temperature of 300 °C, 350 °C and 400 °C respectively. Individual measured values are represented with coloured circles according to the legend below particular figure.

The analysed results show that ram speed does not have any influence on anisotropic flow described by factor  $R_z$ , while initial work-piece temperature and work-piece orientation (loading direction) have significant impact.

In the work-pieces oriented longitudinal, the value of factor  $R_z$  about 1 means that anisotropic flow is not present irrespective of the initial work-piece temperature and ram speed.

In the work-pieces oriented in the 45° anisotropic flow is present but smaller than in the work-pieces oriented transverse. At 300 °C ratio  $R_z = 1.52$  predicts an elliptical shape of the upset work-pieces, but with increasing of initial work-piece temperature significant decreasing of elliptical shape is observed.

In the work-pieces oriented transverse, ratio  $R_z$  shows significant presence of anisotropic flow with dependence on initial work-piece temperature as well. Factor  $R_z$  is decreasing with increasing of the initial work-piece temperature, from value of  $R_z = 2.6$  at 300 °C, following by  $R_z = 1.9$  at 350 °C to  $R_z = 1.6$  at 400 °C at both ram speeds. In this respect, decreasing of the elliptical shape is also noticed.

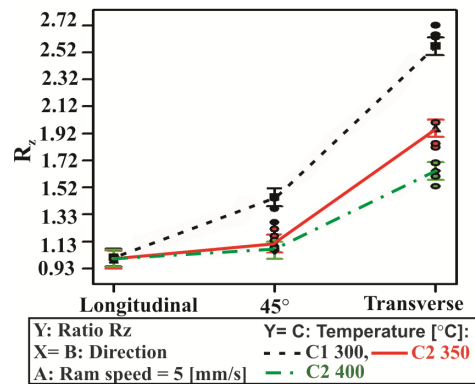


Fig. 9.  $R_z$  ratio at ram speed of 5 mm/s

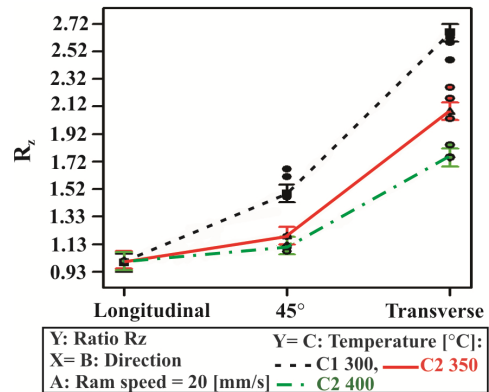


Fig. 10.  $R_z$  ratio at ram speed of 20 mm/s

Within the studied range of input process parameters, mathematical formulations for the calculation of the statistically probable value of anisotropic factor  $R_z$  were proposed for work-

pieces oriented transverse  $R_{z90}$  Eq. (4) and in the  $45^\circ$   $R_{z45}$  Eq. (5), respectively.

$$R_{z90} = 5,24969 + 3,59852 \cdot 10^{-3} \cdot v_r - 9,22595 \cdot 10^{-3} \cdot T + 1,07448 \cdot 10^{-5} \cdot v_r \cdot T. \quad (4)$$

$$R_{z45} = 2,57547 + 1,63637 \cdot 10^{-4} \cdot v_r - 3,95686 \cdot 10^{-3} \cdot T + 1,07448 \cdot 10^{-5} \cdot v_r \cdot T. \quad (5)$$

Predicted *R-squared* ( $R^2$ ) factor is used in regression analysis to indicate how well the proposed mathematical model (equations 4 and 5) predicts responses and fits experimental data. Predicted *R-squared factor* is 0.9577 for both equations which indicates very accurate regression of obtained equations 4 and 5. Obtained equations are also appropriate for mathematical formulation of the  $R_z$  factor within the studied range of input process parameters.

In upsetting, so-called hot cracks at initial work-piece temperatures of  $400^\circ\text{C}$  were also observed. Cracks appeared in longitudinal work-pieces upset through both ram speeds of 5 and 20 mm/s while in the work-pieces oriented in  $45^\circ$  cracks appeared only at ram speed of 20 mm/s as shown in Fig. 11. Specifically, the reduced viscosity of material and exceeded melting point of precipitation phase  $\text{Mg}_{17}\text{Al}_{12}$  ( $427^\circ\text{C}$ ) [2] as well as anisotropy of the structure, especially deposition of  $\text{Mg}_{17}\text{Al}_{12}$  are the main reasons for hot cracking. The risk for hot cracking is even more expressive at higher ram speeds because a greater rise in temperature occurs due to plastic deformation.

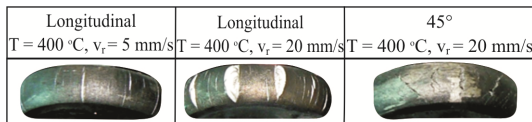


Fig. 11. Cracks at upsetting

### 3.3 Radial Compression Tests

To determining material flow in more complex deformation circumstances, e.g. where work-pieces are compressed in radial directions, radial compression tests (“cigar tests”) were performed, as is a common practice in forging shops. Understanding material flow in conditions where loading force acts in a radial direction perpendicular to extrusion axis is crucial for the filling of die cavities and indirectly affects dies’

cavities and slugs’ design. Moreover, such a deformation state could be a good case study for verifying the precision of FEM codes.

Footprints of radial compression are shown in Fig. 12. Differences in the shapes of footprints show the presence of anisotropic flow.

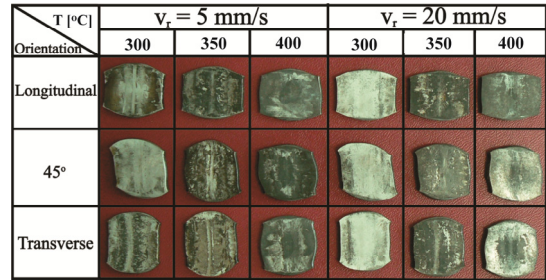


Fig. 12. Footprints at radial compression

Material flow was observed by measuring extension in the direction of work-piece flat planes  $L_1$  and work-piece radii direction  $L_2$  as shown on Fig. 13. The procedure for calculation of equivalent values  $L_1$  and  $L_2$  due to embossment of outer surfaces of radial compressed work-piece was the same as was used for determination diameters  $D_1$  and  $D_2$  at upsetting.

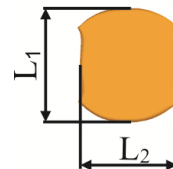


Fig. 13. Measurement of extension  $L_1$  and  $L_2$  at radial compression

Analyses of extension of  $L_1$  and  $L_2$  are illustrated in Figs. 14 and 15. Work-pieces oriented longitudinal show more pronounced extension in radial direction  $L_2$  as in the direction of flat planes  $L_1$ . Dimension  $L_2$  is increasing even more with the increasing of initial work-piece temperature or ram speed, while  $L_1$  is decreasing. In this case, the situation is opposite as with upsetting of work-pieces oriented transverse where anisotropic flow was decreasing with the increasing of initial work-piece temperature.

With the radial compression of work-pieces oriented in the  $45^\circ$ , material flow is quite similar to work-pieces oriented transverse, except that it is slightly more oriented in the direction of  $45^\circ$  regarding the main extrusion axis causing the

oblique final shape (observed from the top perspective). That could be explained by easier formation of gliding planes perpendicular to long-fibre grains as a result of extrusion. It should be also said that measures of  $L_1$  and  $L_2$  do not fully consider anisotropic flow, but is clear in any case that the shapes of radial compressed work-pieces oriented in the  $45^\circ$  are similar to those oriented transverse.

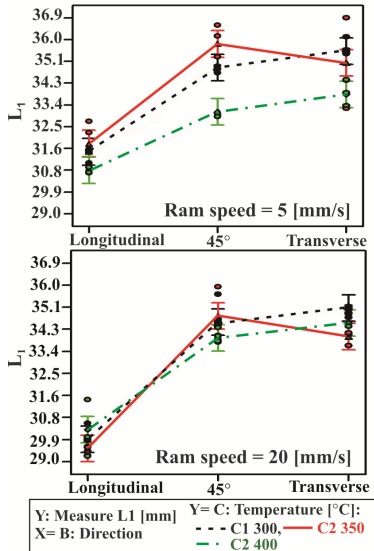


Fig. 14. Statistical analyses of dimension  $L_1$  for ram speed of 5 mm/s and ram speed of 20 mm/s

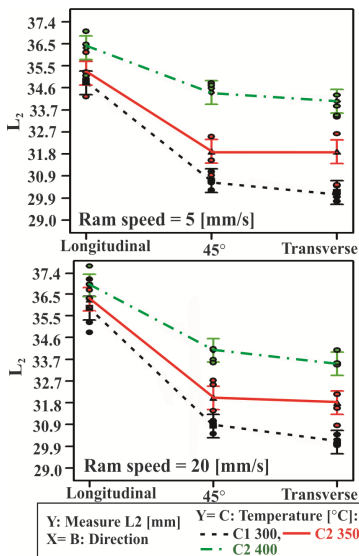


Fig. 15. Statistical analyses of dimension  $L_2$  for ram speed of 5 mm/s and ram speed of 20 mm/s

At radial compression of work-pieces oriented transverse at  $300^\circ\text{C}$ , material flows more uniformly in both directions  $L_1$  and  $L_2$ . However, with increasing of initial work-piece temperature, material flow becomes more superior in the direction of work-piece radial surface  $L_2$ .

Deformation behaviour in the radial compression also provided crack formation, but not to the extent to that happened in upsetting. Only in work-pieces oriented in the  $45^\circ$  did cracks appear in work-piece radial surfaces, as shown on Fig. 16.



Fig. 16. Cracking at radial compression

#### 4 THE MOST IMPORTANT CONCLUSIONS

The performed analyses give some very important explanations of plastic deformation behaviour of magnesium wrought alloy AZ80.

The basic influence on material flow, the formation of an elliptical shape at upsetting or differences in material flow in radial compression, during deformation have strong grain orientation as a result of pre-extrusion process. From analysed results, it is clear that formation of gliding planes is easier perpendicular to long grains rather than in longitudinal direction parallel to long grains.

In terms of the most important contributions to industrial practice, the following findings can be highlighted:

- Ram speed between 5 and 20 mm/s does not have remarkable influence on anisotropic flow regardless of the work-piece placement or work-piece orientation (loading direction).
- The most optimal initial work-piece temperature for isothermal forging on hydraulic press is  $350^\circ\text{C}$ ; however, lower initial work-piece temperatures would be recommended for forging on screw presses or hammers, because larger rises in temperature at relatively high strain rates are expected. As has also been experimentally detected, at an initial work-piece temperature of  $400^\circ\text{C}$  hot cracks already appeared at quite slow strain rates.

- The hydraulic press machine was recognised as highly recommended for the forging of magnesium wrought alloys since slow strain rates suitable for the forging of magnesium alloys could be achieved with ram speed control.

The present study represents some new insights into magnesium forging technology with significant potential for practical use and further investigation. The main goal for further investigation should be focused on reliable numerical simulations of bulk forming of magnesium alloys.

For complete consideration of magnesium deformation characteristic with numerical simulations, attention should be paid on development of finite element models capable to predict and calculate texture changes of h. c. p. polycrystalline materials.

Further efforts should be made on the field of testing procedures for determination of anisotropic variables for any type of anisotropic yielding law.

The final stage results of present study could be used as a case study for testing the capabilities and accuracy of numerical simulations of anisotropic material flow.

## 5 ACKNOWLEDGEMENTS

The represented research work is a part of a Collective Research Project MagForge – Magnesium Forged Components for Structural Lightweight Transport Applications with Contract no.: COLL-CT-2006-030208 founded by EC as a 6FP project.

## 6 REFERENCES

- [1] Kurz, G., Sillekens, W.H., Swiostek, J., Letzig, D. (2007). Alloy development and processing for the European project MagForge. *Proceedings of the 15<sup>th</sup> Magnesium Automotive and User Seminar*, p. 27-28.
- [2] Kurz, G., Clauw, B., Sillekens, W.H., Letzig, D. (2009). Die Forging of the Alloys AZ80 and ZK60. *TMS – Magnesium Technology*, p. 197-202.
- [3] Kocańda, A., Czyżewski, P. (2008). Experimental and numerical analysis of side forces in a forging die. *Strojniški vestnik – Journal of Mechanical Engineering*, vol. 54, no. 4, p. 274-279.
- [4] Cazacu, O., Plunkett, B., Barlat, F. (2006). Orthotropic yield criterion for hexagonal closed packed metals. *International Journal of Plasticity*, vol. 22, p.1171-1194.
- [5] Lass, J.F., Bach, F.W., Schaper, M. (2005). Adapted Extrusion Technology for Magnesium Alloys. *TMS – Magnesium Technology*, p. 15-17.
- [6] Graff, S., Brocks, W., Steglich, D. (2007). Yielding of magnesium: From single crystal to polycrystalline aggregates. *International Journal of Plasticity*, vol. 23, p. 1957-1978.
- [7] Kurz, G., Letzig, D. Delivery presentation – Progress on WP1 material development, from <http://www.magforge.eu>, accessed on 2007-06-26.
- [8] Montgomery, D.C. (2001). *Design and Analysis of Experiments*, 5<sup>th</sup> Edition. John Wiley & Sons, New York. p. 363–387.
- [9] ATOS User Information. ATOS II/II Small Object Hardware, from <http://www.gom.com>, accessed on 2008-01-31.
- [10] Kobold, D., Pepelnjak, T., Gantar, G., Kuzman, K. (2009). Analyses of material properties of magnesium alloys on warm forging processes. *Proceedings of the 8<sup>th</sup> International Conference on Magnesium Alloys and their Applications*, p. 113-119.
- [11] Lekhnitskii, S.G. (1989). *Theory of Elasticity of an Anisotropic Body*. Moscow – MIR Publishers. p. 15-78, (English translation of supplemented Russian edition from year 1977).
- [12] Aleksandrović, S., Stefanović, M., Adamović, D., Lazić, V. (2009). Variation of normal anisotropy ratio "r" during plastic forming. *Strojniški vestnik – Journal of Mechanical Engineering*, vol. 55, no. 6, p. 392-399.
- [13] Banabic, D., Bunge, H.J., Pohlandt, K., Tekkaya, A.E. (2000). *Formability of Metallic Materials: Plastic Anisotropy, Formability Testing, Forming Limits*. Springer Verlag. p. 86-107.